Experimental and theoretical study of topology and electronic correlations in PuB_{4}

Hongchul Choi, Wei Zhu, S. K. Cary, L. E. Winter, Zhoushen Huang, R. D. McDonald, V. Mocko, B. L. Scott, P. H. Tobash, J. D. Thompson, S. A. Kozimor, E. D. Bauer, Jian-Xin Zhu, and F. Ronning

Phys. Rev. B **97**, 201114 — Published 29 May 2018

DOI: 10.1103/PhysRevB.97.201114

Experimental and Theoretical Study of Topology and Electronic Correlations in PuB_4

Hongchul Choi,[1] Wei Zhu,[1] S. K. Cary,[1] L. E. Winter,[1] Zhoushen Huang,[1] R.D. McDonald,[1] V. Mocko,[1] B. L. Scott,[1] P. H. Tobash,[1] J. D. Thompson,[1] S. A. Kozimor,[1] E. D. Bauer,[1] Jian-Xin Zhu,[1] and F. Ronning[1]

[1]*Los Alamos National Laboratory, Los Alamos, NM 87545, USA*

We synthesize single crystals of PuB_4 using an Al-flux technique. Single crystal diffraction data provide structural parameters for first principles density functional theory (DFT) calculations. By computing the density of states, the Z_2 topological invariant using the Wilson loop method, and the surface electronic structure from slab calculations, we find that PuB_4 is a non-magnetic strong topological insulator with a band gap of 254 meV. Our magnetic susceptibility, heat capacity and resistivity measurements are consistent with this analysis, albeit with a smaller gap of 35 meV. DFT plus dynamical mean-field theory calculations show that electronic correlations reduce the size of the band gap, and provide better agreement with the value determined by resistivity. These results demonstrate that PuB_4 is a promising actinide material to investigate the interplay of electronic correlations and non-trivial topology.

PACS numbers: 71.18.+y,71.27.+a,72.15.Qm

The consequences of non-trivial topologies in materials have attracted widespread interest in recent years[1,2]. Insulators with strong spin-orbit coupling (SOC) can create a band inversion that necessarily leads to the presence of protected surface states. For materials where electronic correlations are weak, first principles electronic structure approaches have been incredibly powerful in accurately predicting their topology and the corresponding surface states. In the presence of strong electronic correlations, however, new phenomena are anticipated, but are difficult to realize in actual materials[3]. f-electron materials possess both strong spin-orbit coupling and strong electronic correlations and are excellent candidates to explore the combination of non-trivial topologies and correlated electron behavior.

SmB_6 is the most strongly compelling example of a correlated topological insulator, but its small energy scales have resulted in a debate as to the influence of correlations on the proposed surface state[4,5]. Elemental plutonium and its compounds are known to have strong electronic correlations with larger energy scales than their $4f$ counterparts, and could be helpful in this regard[6,7]. Indeed, PuTe and PuB_6 are predicted to be correlated topological insulators, but lack experimental validation[8,9]. In this work, we have synthesized single crystals of PuB_4. Our electronic structure calculations indicate this material is also a strong topological insulator, and our transport and thermodynamic measurements support the electronic state proposed by these first principles calculations. The band gap measured by transport, however, is an order of magnitude smaller than predicted by DFT calculations. Similar to SmB_6, our DFT plus dynamical mean-field theory (DFT+DMFT) calculations suggest this reflects the presence of electronic correlations. This work demonstrates that PuB_4 is a compelling candidate to investigate the influence of electronic correlations on a topological insulator.

Single crystals of PuB_4 were synthesized with plutonium metal[10] and boron powder using aluminum flux[11]. The crystal structure determined by single crystal x-ray

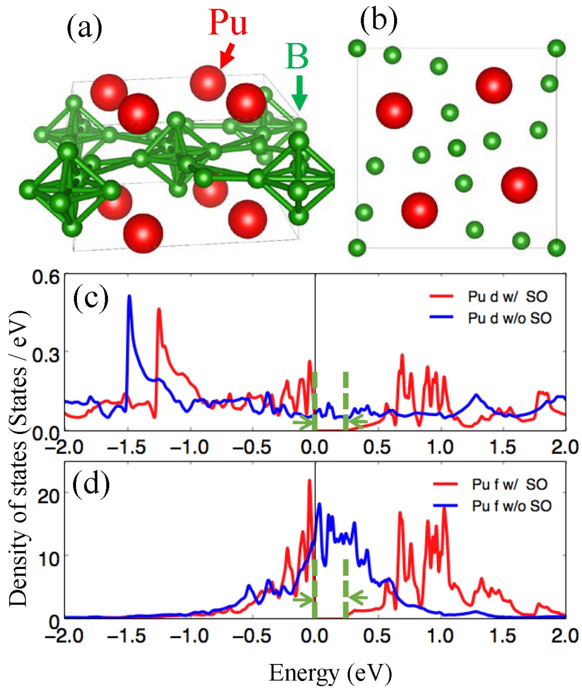

FIG. 1. (color online) (a) The crystal structure of PuB_4. (b) Top view of the structure shows the non-symmorphic symmetry, generated by the combined symmetry of mirror and translation symmetries. The local density of states (LDOS) in PuB_4 with (red) and without (blue) SOC are calculated with the DFT method for (c) the Pu-d and (d) the Pu-f states. The green arrows represent the gap formation with SOC.

diffraction[12,13] presented in Fig. 1 with a = 7.109 Å and c =4.009 Å is in good agreement with previous work on polycrystalline samples[14–16]. A crystallographically unique Pu atom (shown as blue circles in Fig. 1) is surrounded by three different types of boron atoms, distinguished by red (B1), green (B2), and yellow (B3) circles with Pu-Pu distances longer than typical Pu-Pu bond lengths[17]. From the boron perspective, the solid is best described as having two different boron structure types; B_6-distorted octahedra (yellow and red) and B_2 linking units (green). Unlike the cubic symmetry of the proposed topological insulators $R B_6$ (R= Sm, Pu)[18], PuB_4 has tetragonal symmetry, with four formula units (f.u.) in the primitive unit cell. The structure possesses nonsymmorphic symmetries, which impose additional constraints on the electronic structure.

The density of states (DOS) is calculated using density functional theory (DFT) using the generalized gradient approximation as implemented with the WIEN2K code[19,20] (see supplemental information). Figures 1 (c) and (d) demonstrate how the spin-orbit coupling modifies the metallic ground state (blue lines) to an insulating state (red lines). The band gap when including SOC is 254 meV, which is one order of magnitude larger than the tens of meV gaps in $R B_6$ (R=Sm, Pu)[8,21,22]. Clearly, SOC is essential for establishing the insulating ground state in PuB_4. Additionally, the near E_F spectral weight is dominated by Pu-d and Pu-f states, which suggests that electronic correlations may play a role in the physics of PuB_4.

The electronic band structure including SOC is presented in Fig. 2. At all k-points two-fold degeneracies are required by the combined time-reversal and inversion symmetries of the non-magnetic lattice. The bandstructure along R-A and M-X demonstrates the additional constraint in momentum space forced by the nonsymorphic symmetry in real space[23]. Along these paths, when k_x or $k_y = \pi$, a four-fold degeneracy occurs. At R, A, M, and X, two different branches merge into one branch to render the four-fold degeneracy.

To identify the topology of PuB_4, we first construct a tight binding model from the DFT calculation with Pu f, Pu d, B p and B s orbitals using the maximally localized Wannier function method (see[11,24–27]). As shown in Fig. 2, the tight binding model accurately reproduces the low energy ($E_F \pm 2$ eV) electronic structure of PuB_4. Using this tight binding model we investigate the topological property of PuB_4 by the evolution, or "flow", of the Wannier centers in momentum space, from which quantized topological indices (the first Chern number or Z_2 number) can then be extracted graphically[28]. Figures 2 (b) and (c) show the Wilson flow in the k_z=0 and π planes, respectively. The minimum number of crossings of any horizontal reference line in Fig. 2 (b) and (c) are 1 and 0, respectively. The three-dimensional Z_2 index is determined by whether the summation of these two numbers is even or odd. The odd number for the Wilson flow asserts that PuB_4 is a so-called strong topological insulator.

The Wilson flow calculation together with the space group symmetry of the crystal also informs us about the properties of the topologically protected surface states. The single crossing found in Fig. 2 (b) means an odd number of exchanges of Kramers partners in the k_z=0 plane, while there will be an even number of exchanges for $k_z = \pi$ (Fig. 2 (c)). Since the k_z =0 plane has effectively two X points, the exchange occurs at either Γ or M. The non-symmorphic symmetry, however, requires a double degeneracy at the M point so we can conclude that the exchange must occur at Γ. Therefore, in a slab geometry perpendicular to the z axis, a topologically protected Dirac cone will emerge on the surface at $\bar{\Gamma}$ of the surface Brillouin zone.

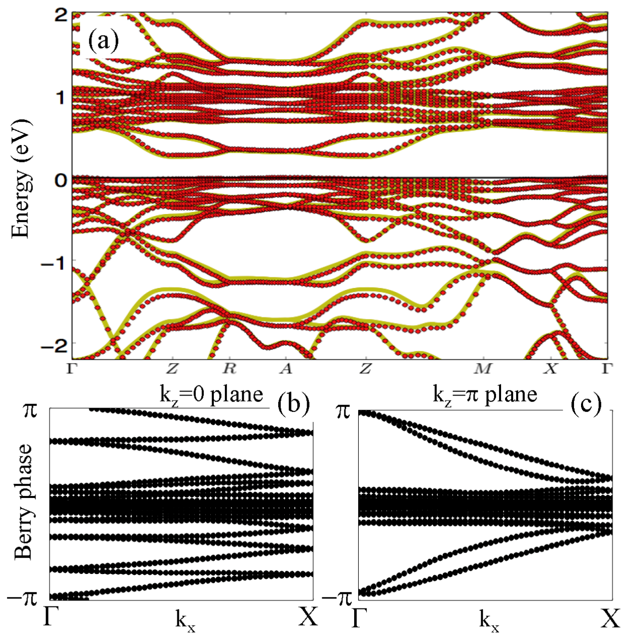

FIG. 2. (color online) Comparison of the bandstructures from the DFT calculation (red circles) with the tight binding model (yellow line). The black line at 0 eV represents the Fermi level. Γ, Z, R, A, M, and X represent (0,0,0), (0,0,π),(π,0,π),(π,π,π),(π,π,0),(π,0,0) in reciprocal space. (b,c) The evolution lines of the Wannier centers for PuB_4. The evolution lines cross a horizontal line an odd number of times (b) in the $k_z = 0$ plane and an even number of times (c) in the $k_z = \pi$.

To visualize the topologically protected surface state we computed the electronic structure using a slab geometry. 1x1x10 supercells were prepared with and without open boundary conditions at the top and bottom of the supercell. Due to the computational cost, a reduced basis with only Pu f and Pu d states was employed to compute the slab geometry. We confirmed that the Wilson loop calculation with the reduced basis set possesses the same topology as in Fig. 2 (b) and (c). We used the same value of E_F for the supercells as calculated in the primitive unit cell. Band-folding along the k_z axis results in a complicated and dense bandstructure. With periodic boundary conditions as in the bulk crystal the insulating phase is maintained (Fig. 3 (a)). In the presence of open boundary conditions, however, Fig. 3 (b) illustrates the Dirac cone arising at Γ, as expected from the Wilson flow calculation. Due to the existence of surfaces at the

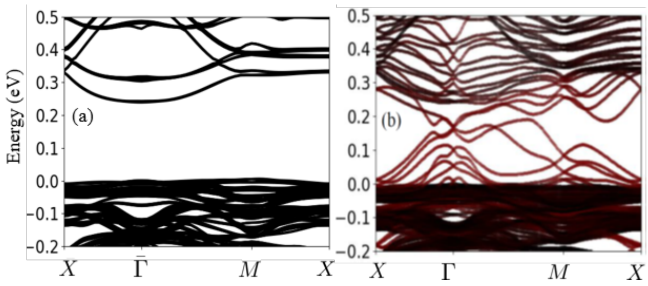

FIG. 3. (color online) (a) The 1x1x10 supercell bandstructure and (b) its surface states of PuB_4 on (001) surface. X,Γ, M in (a) are (π,0,0),(0,0,0), (π,π,0) in the supercell Brillouin zone, and $\bar{X}$,$\bar{\Gamma}$, $\bar{M}$ in (b) are (π,0),(0,0), (π,π) in the surface Brillouin zone perpendicular to z-axis. Red bands emphasize surface derived states.

top and bottom of the slab, the Dirac point realizes a four-fold degeneracy. We note that several trivial surface states also manifest due to the large number of Pu f and d orbitals at the surface. Both calculations of the Wilson flow and the surface electronic bandstructure establish a non-trivial topology of PuB_4 using a DFT approach.

Validating the DFT calculations, experiments demonstrate that PuB_4 is a non-magnetic insulator. Magnetic susceptibility measurements are shown in Fig. 4 (a) for a 42.5 mg sample composed of an aggregate of many crystals. The lack of local magnetic moments is reflected by the small and weak temperature dependence of the magnetic susceptibility in agreement with previous studies and similar to that found in other paramagnetic insulators[29]. The small positive value may be a result of a Van Vleck contribution or from in-gap states At low temperatures there is a small increase most likely originating from a minor magnetic impurity of unknown origin. Heat capacity measurements in Fig. 4 (b) reveal a tiny residual electronic term. We fit the specific heat to the expression: $C/T = \gamma + \beta T^2$ below 11 K. This yields $\gamma = 2.5$ mJ/mol K^2 and a Debye temperature $\theta_D = 430$ K from the formula $\theta_D = (12\ \pi^4 nR/(5\beta))^{1/3}$, where R is the gas constant and $n = 5$ for the number atoms per formula unit. The presence of a residual γ term is much smaller than what is found in SmB_6[30,31], which we believe reflects localized in gap states of unknown origin. A large Wilson ratio $R_W \sim\ 11$ in this non-magnetic compound implies that the susceptibility and linear specific heat coefficient have different origins.

The insulating nature of PuB_4 is confirmed by the resistivity measurements shown in Fig. 5. At temperatures below roughly 100 K the resistivity rolls over and begins to saturate. Presently, it is impossible to determine whether the resistivity saturation is a consequence of in-gap states as observed in many Bi_2Se_3 samples[32] or from a metallic surface state as observed in SmB_6 and some high quality Bi_2Se_3 thin films[33–35]. We were unable to vary the thickness sufficiently systematically to draw a conclusion regarding this point. As shown in the inset of Fig. 5, we fit the resistivity to a parallel conduction model $\rho = (1/\rho_0 + 1/(\rho_b \exp(\Delta/k_B T)))^{-1}$ with one channel corresponding to a temperature independent metallic channel that would arise from a surface or impurity band and a second channel corresponding to the activated bulk behavior. This fit gives $\Delta = 35$ meV for the bulk behavior, which is significantly smaller than the band gap determined by DFT. The resistivity at the lowest temperatures does not saturate as quickly as the simple two channel model would indicate. This may reflect some degree of localization or other correlation effect on the low temperature transport, which requires further investigation.

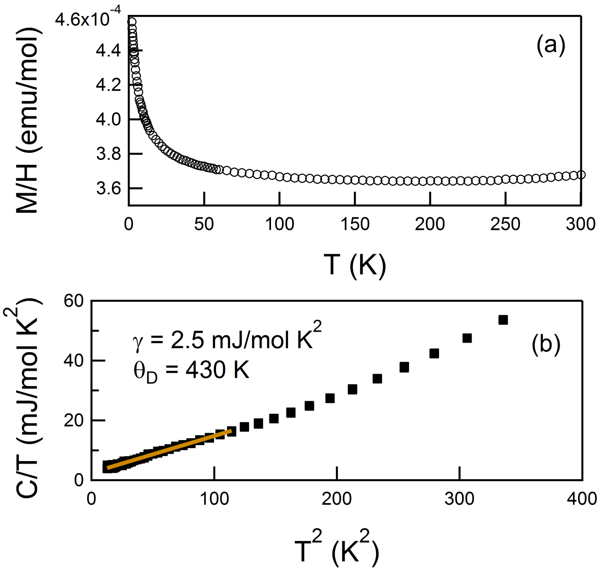

FIG. 4. (color online) (a) Magnetization (ΔM) at 5 T divided by the magnetic field versus the temperature. (b) Low temperature specific heat divided by temperature versus the square of the temperature. The solid line is a linear fit to the data, whose y-intercept provides the electronic contribution characterized by γ, while the slope provides the phonon contribution characterized by θ_D.

These calculations and measurements on PuB_4 show that it has properties similar to those of SmB_6, but with an order of magnitude larger energy scale in the tetraboride (see Table 1). In SmB_6, the DFT determined band gap is ≈ 15 meV[21,22], which is larger than the gap of ≈ 2.3 meV measured by resistivity[36]. Below $T^* \approx$ 4 K there is a crossover in SmB_6 to a metallic surface dominated regime[33,37]. In PuB_4, both the DFT and resistively determined gaps are roughly an order of magnitude larger than in SmB_6, and the crossover to a resistively saturating regime occurs roughly 25 times higher in temperature. Additionally, the magnetic susceptibility and residual specific heat values are both roughly an order of magnitude smaller in PuB_4 relative to SmB_6 as one might expect if the energy scales are an order of magnitude larger. This comparison suggests that PuB_4 is an analog of SmB_6 with larger energy scales, which

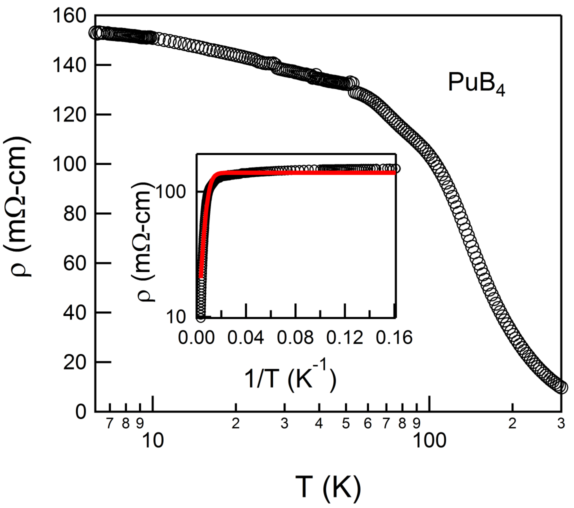

FIG. 5. (color online) Resistivity of a PuB_4 single crystals versus temperature. The inset shows a plot versus inverse temperature, where the solid red line is a fit to a two channel model yielding a bulk gap of 35 meV as described in the text.

TABLE I. Comparison of several properties of PuB_4 versus SmB_6. Values for PuB_4 are from this work, while values for SmB_6 come from the references given in the last column.

	PuB_4	SmB_6	refs
Δ_{DFT} (meV)	254	14-23	21,22
Δ_{ρ} (meV)	35	2.3	36
T^* (K)	100	4	33,37
χ_o (emu/mol)	3.6x10^{-4}	3x10^{-3}	36
γ_{resid} (mJ/molK^2)	2.5	7-30	30,31

may ease interrogation of its surface states with ARPES and/or STM.

In SmB_6, strong electronic correlations renormalize the DFT determined band gap from $\approx$ 15 meV to the experimentally measured gap of $\approx$ 2.3 meV without changing the topology of the system[38–40]. To see if correlations play a similar role in PuB_4 we investigate the gap size using DFT+DMFT, where an on-site Coulomb interaction (U) is added to the f-electron[11,41,42]. Table II shows the theoretically-determined gap size as a function of U. The value at $U = 0.0$ eV corresponds to the gap calculated by DFT, shown in Fig. 1. Since we use the strong-coupling based impurity solver, we could not describe the states near the DFT ground state with negligible U. Typical U values for Pu are 4 - 4.5 eV[6,43–45], and in that range self-consistency could be achieved. As a function of U from 3.5 eV to 4.5 eV, the computed band gaps decrease from 15.2 meV to 10.3 meV. By including the effects of correlations on the Pu $5f$ electrons, the DFT+DMFT band gap is reduced by one order of magnitude relative to the overestimated DFT band gap, which supports the notion that electronic correlations play an important role in PuB_4. Furthermore, we note that a spin-polarized

TABLE II. Variation of the gap between valence and conduction bands as a function of U (on-site Coulomb interaction).

Correlation effect on the gap size					
U (eV)	0	3.5	4.0	4.5	Experiment
gap size (meV)	253.6	15.2	13.2	10.3	35

DFT calculation without U incorrectly predicts a magnetic ground state in contradition with the experimental results, thereby necessitating the need to include correlations. Because the insulating phase is maintained throughout the DFT+DMFT calculations, the robustness of the non-trivial topology is presumed.

In summary, transport and thermodynamic measurements on single crystals of PuB_4 demonstrate that it is a non-magnetic insulator. This is consistent with DFT calculations, which suggest that PuB_4 is a strong topological insulator. This may explain the saturating resistivity behavior at low temperatures. The presence of electronic correlations are revealed by the renormalization of the band gap as measured by resistivity, and reproduced in our DFT+DMFT calculations. Experimentally, PuB_4 shares many similarities with SmB_6, but with a larger energy scale. Our results suggest that PuB_4 is a promising candidate to explore the effect of electronic correlations in a topologically non-trivial material. Spectroscopic probes, such as ARPES and STM, will be particularly valuable to understand this interplay.

ACKNOWLEDGMENTS

We immensely appreciate Zach Fisk and Priscila Rosa for assistance with the crystal growth and gratefully acknowledge the Los Alamos National Laboratory Laboratory Directed Research and Development (LDRD-DR 20160085DR) for support (Choi, Zhu, Winter, Huang, McDonald, Tobash, Thompson, Kozimor, Bauer, Zhu, Ronning). Portions of this work were also supported by the LDRD office through a Darleane Christian Hoffman Distinguished Postdoctoral Fellowship (Cary). We also acknowledge support through the LANL Heavy Element Chemistry Program that is funded by the Division of Chemical Sciences, Geosciences, and Biosciences, Office of Basic Energy Sciences, U.S. Department of Energy (Mocko, Scott). Los Alamos National Laboratory is operated by Los Alamos National Security, LLC, for the National Nuclear Security Administration of U.S. Department of Energy (contract DE-AC52-06NA25396).

[1] M. Z. Hasan and C. L. Kane, Rev. Mod. Phys. 82, 3045 (2010).

[2] Xiao-Liang Qi and Shou-Cheng Zhang, Rev. Mod. Phys.

83, 1057 (2011).
[3] e.g. A. Stern, Annu. Rev. Condens. Matter Phys., 7, 349 (2016).
[4] M. Dzero, K. Sun, V. Galitski, and P. Coleman, Phys. Rev. Lett. 104, 106408 (2010).
[5] M. Dzero, J. Xia, V. Galitski, and P. Coleman, Annu. Rev. Condens. Matter Phys. 7, 249 (2016).
[6] J. H. Shim, K. Haule, G. Kotliar, Nature 446, 513-516 (2007).
[7] C. H. Booth, Yu Jiang, D.L. Wang, J.N. Mitchell, P.H. Tobash, E.D. Bauer, M.A. Wall, P.G. Allen, D. Sokaras, D. Nordlund, T.-C. Weng, M.A. Torrez, and J.L. Sarrao, PNAS 109, 10205-10209 (2012).
[8] X. Deng, K. Haule, and G. Kotliar, Phys. Rev. Lett. 111, 176404 (2013).
[9] X. Zhang, H. Zhang, J. Wang, C. Felser, S.-C. Zhang, Science 335, 1464 (2012).
[10] National Nuclear Data Center. Brookhaven National Laboratory. http://www.nndc.bnl.gov/chart/ (Feburary 6, 2018).
[11] Supplemental Material
[12] S.K. Cary, K.S. Boland, J.N. Cross, S.A. Kozimor, and B.L. Scott, Polyhedron, **126**, 220 (2017).
[13] A. Spek, J. Appl. Cryst., **36**, 7 (2003).
[14] B.J. McDonald and W.I. Stuart, Acta Cryst. 13, 447 (1960).
[15] H. A. Eick, Inorganic Chemistry 4, 1237 (1065).
[16] P. Rogl and P. Potter, J Phase Equilib 18, 467 (1997).
[17] F.J. Espinosa, P. Villela, J.C. Lashley, S.D. Conradson, L.E. Cox, R. Martinez, B. Martinez, L. Morales, J. Terry, and R.A. Pereyra, Phys. Rev. B, **63**, 174111 (2001)
[18] Z. Fisk, P. H. Schmidt, and L.D. Longinotti; Mat. Res. Bull. **11**, 1019 (1976).
[19] P. Blaha, K. Schwarz, G. Madsen, D. Kvasicka, and J. Luitz, WIEN2K, An Augmented Plane Wave + Local Orbitals Program for Calculating Crystal Properties (Technical University of Vienna, Vienna, 2001).
[20] J. P. Perdew, K. Burk Properties (Technical University of Vienna, Vienna, 2001).
[21] A. Yanase and H. Harima: Prog. Theor. Phys. Suppl. 108 (1992) 19.
[22] V. N. Antonov, B. N. Harmon, and A. N. Yaresko: Phys. Rev. B 66, 165209 (2002)
[23] S. M. Young and C. L. Kane, Phys. Rev. Lett. 115, 126803 (2015)
[24] J. Kunes, R. Arita, P. Wissgott, A. Toschi, H. Ikeda, and K. Held, Comp. Phys. Commun. **181**, 1888 (2010).
[25] N. Marzari and D. Vanderbilt, Phys. Rev. B **56**, 12847 (1997).
[26] I. Souza, N. Marzari and D. Vanderbilt, Phys. Rev. B **65**, 035109 (2001).
[27] A.A. Mostofi, J.R. Yates, G. Pizzi, Y.S. Lee, I. Souza, D. Vanderbilt, and N. Marzari Comput. Phys. Commun. **185**, 2309 (2014).
[28] Rui Yu, Xiao Liang Qi, Andrei Bernevig, Zhong Fang, and Xi Dai, Phys. Rev. B **84**, 075119 (2011)
[29] J. L. Smith and H. H. Hill, Magnetism in neptunium borides, AIP Conference Proceedings 24, 382 (1975).
[30] T. Kasuya, K. Takegahara, T. Fujita, T. Tanaka, and E. Bannai, J. Phys. (Paris) 40 (1979) C5-308
[31] W. A. Phelan, S. M. Koohpayeh, P. Cottingham, J.W. Freeland, J. C. Leiner, C. L. Broholm, and T. M. McQueen, Phys. Rev. X 4, 031012 (2014)
[32] S. Barua and K. P. Rajeev AIP Advances 4, 017135 (2014)
[33] D. Kim, S. Thomas, T. Grant, J. Botimer, Z Fisk, and J. Xia, Sci. Rep. 3, 3150 (2013)
[34] D.J. Kim, J. Xia, and Z. Fisk, Nature Materials, **13**, 466 (2014).
[35] A. A. Taskin, Satoshi Sasaki, Kouji Segawa, and Yoichi Ando, Phys. Rev. Lett. 109, 066803 (2012); Namrata Bansal, Young Seung Kim, Matthew Brahlek, Eliav Edrey, and Sheongshik Oh, Phys. Rev. Lett 109, 116804 (2012)
[36] Menth, A. and Buehler, E. and Geballe, T. H. Phys. Rev. Lett. 22, 295 (1969)
[37] Allen, J. W. and Batlogg, B. and Wachter, P. Phys. Rev. B 20, 4807 (1979)
[38] T. Takimoto, J. Phys. Soc. Jpn. 80, 123710 (2011).
[39] F. Lu, J. Z. Zhao, H.Weng, Z. Fang, and X. Dai, Phys. Rev. Lett. 110, 096401 (2013).
[40] J. Kim, K. Kim, C.-J. Kang, S. Kim, H.C. Choi, J.-S. Kang, J.D. Denlinger, and B.I. Min, Phys. Rev. B 90, 075131 (2014)
[41] G. Kotliar, S. Y. Savrasov, K. Haule, V. S. Oudovenko, O. Parcollet, and C. A. Marianetti, Rev. Mod. Phys. **78**, 865 (2006).
[42] K. Haule, C.-H. Yee, and K. Kim, Phys. Rev. B **81**, 195107 (2010)
[43] M.-T. Suzuki and P.M. Oppeneer, Phys. Rev. B **80**, 161103(R) (2009).
[44] J.-X. Zhu, P.H. Tobash, E. D. Bauer, F. Ronning, B. L. Scott, K. Haule, G. Kotliar, R.C. Albers, and J.M. Wills, EPL 97 57001 (2012)
[45] J.-X. Zhu, R. C. Albers, K. Haule, G. Kotliar, and J. M. Wills, Nat. Commun. 4, 2644 (2013)